Free Radical Biology and Medicine xxx (xxxx) xxx–xxx

Contents lists available at ScienceDirect

Free Radical Biology and Medicine

journal homepage: www.elsevier.com/locate/freeradbiomed

Pro-oxidant and pro-inflammatory effects of glycated albumin on cardiomyocytes

Alma Martinez Fernandez[a], Luca Regazzoni[b], Maura Brioschi[a,*], Erica Gianazza[a], Piergiuseppe Agostoni[a,c], Giancarlo Aldini[b], Cristina Banfi[a]

[a] Centro Cardiologico Monzino, IRCCS, Milan, Italy
[b] Department of Pharmaceutical Sciences, University of Milan, Milan, Italy
[c] Department of Clinical Sciences and Community Health, Cardiovascular Section, University of Milan, Milan, Italy

ARTICLE INFO

Keywords:
Glycated albumin
Cardiomyocytes
Oxidative stress
Inflammatory response

ABSTRACT

Human serum albumin (HSA) is the most abundant circulating protein in the body and presents an extensive range of biological functions. As such, it is prone to undergo post-translational modifications (PTMs). The non-enzymatic early glycation of HSA, one of the several PTMs undergone by HSA, arises from the addition of reducing sugars to amine group residues, thus modifying the structure of HSA. These changes may affect HSA functions impairing its biological activity, finally leading to cell damage.

The aim of this study was to quantitate glycated-HSA (GA) levels in the plasma of heart failure (HF) patients and to evaluate the biological effects of GA on HL-1 cardiomyocytes.

Plasma GA content from HF patients and healthy subjects was measured by direct infusion electrospray ionization mass spectrometry (ESI-MS). Results pointed out a significant increase of GA in HF patients with respect to the control group ($p < 0.05$). Additionally, after stimulation with GA, proteomic analysis of HL-1 secreted proteins showed the modulation of several proteins involved, among other processes, in the response to stress. Further, stimulated cells showed a rapid increase in ROS generation, higher mRNA levels of the inflammatory cytokine interleukin-6 (IL-6) and tumor necrosis factor alpha (TNF-α), and higher levels of the oxidative 4-HNE-protein adducts and carbonylated proteins.

Our findings show that plasma GA is increased in HF patients. Further, GA exerts pro-inflammatory and pro-oxidant effects on cardiomyocytes, which suggest a causal role in the etiopathogenesis of HF.

1. Introduction

Human serum albumin (HSA) is the most abundant circulating protein in the body. Besides its well-known oncotic function, it has an extensive range of physiological and pharmacological functions that may be relevant under physiological circumstances and in disease [1].

It plays an important defensive role in oxidative stress, exerts immunomodulatory, anti-inflammatory, and anti-coagulant effects; it is a crucial part of the endothelial surface, and contributes to the maintenance of the normal capillary permeability and endothelial stabilization (reviewed in Ref. [1]). Further, a plethora of drugs has been determined to bind in specific sites of albumin, so that albumin has a fundamental drug-carrier role which interferes with drugs efficacy and availability at target organs [2].

Because of its long half-life (about 21 days) compared with other proteins and its high concentration in the circulatory system, serum

Abbreviations: **4-HNE**, 4-hydroxy-2-nonenal; **ACN**, acetonitrile; **AGEs**, advanced glycation end products; **CML**, carboxymethyl lysine; **CVD**, cardiovascular diseases; **DMSO**, dimethyl sulfoxide; **DNP**, dinitrophenol; **DNPH**, 2,4-dinitrophenylhydrazine; **ELISA**, enzyme-linked immunosorbent assay; **eNOS**, endothelial nitric oxide synthase; **ESI**, electrospray ionization; **FA**, formic acid; **GADPH**, glyceraldehyde 3-phosphate dehydrogenase; **GA**, glycated human serum albumin; **GLM**, general linear model; **HF**, heart failure; **HSA**, human serum albumin; **HSA-SH**, mercaptoalbumin; **HSP**, heat shock protein; **IL-6**, interleukin-6; **LC**, liquid chromatography; **MS**, mass spectrometry; **MTT**, 3-(4,5-dimethylthiazol-2-yl)-2,5-diphenyltetrazolium bromide; **NADPH**, nicotinamide adenine dinucleotide phosphate; **NF-κB**, nuclear factor kappa-light-chain-enhancer of activated B cells; **Nrf2**, nuclear factor (erythroid-derived 2)-like 2; **NYHA**, New York Heart Association; **PCR**, polymerase chain reaction; **PGC1**, peroxisome proliferator-activated receptor gamma coactivator 1; **PTMs**, post-translational modifications; **qRT-PCR**, real-time quantitative PCR; **ROS**, reactive oxygen species; **SDS-PAGE**, sodium dodecyl sulfate polyacrylamide gel electrophoresis; **TNF-α**, tumor nrecrosis factor alpha; **UPLC**, Ultra performance liquid chromatography

* Corresponding author. Monzino Cardiologic Center IRCCS, 20138, via Parea, 4, Milan, Italy.
E-mail address: maura.brioschi@ccfm.it (M. Brioschi).

https://doi.org/10.1016/j.freeradbiomed.2019.06.023
Received 19 December 2018; Received in revised form 13 June 2019; Accepted 19 June 2019

albumin is a plasmatic protein that is highly sensitive to post-translational modifications (PTMs), such as glycation.

Non-enzymatic glycation is indeed one of the underlying modifications that can modify its native secondary and tertiary structure [3]. In this process, also known as the Maillard reaction, free amine groups of albumin are initially attached by glucose or derivatives to reversibly form a Schiff base product, followed by the formation of a stable fructosamine residue by Amadori rearrangement. This is the early glycation process: Schiff's base and fructosamine (Amadori product) have been called early glycation adducts. Further modifications in these early stage glycation products, such as rearrangement, oxidation, polymerization, and cleavage give rise to irreversible conjugates, called advanced glycation end products (AGEs) [4].

Non-enzymatic glycation occurs in normal conditions, but HSA is typically 2–3 times more glycated than the rest of the serum proteins in hyperglycaemic condition [3].

Several *in vitro* studies have shown the implication of glycated albumin, mainly AGE-albumin, in cardiovascular diseases (CVD): for example, platelets are activated by both irreversibly and reversibly glycated albumin, thus promoting CVD development [5]; in endothelial cells glycated albumin enhanced ROS production by activating multiple signaling pathways [6]. Glycated albumin can also trigger damaging effects *in vitro* and *in vivo* on hepatic cells [7], all features that contribute to the increased mortality of diabetic patients [8]. Finally, bovine glycated albumin stimulates cardiomyocyte ROS production, which results in NF-κB activation and upregulation of atrial natriuretic factor mRNA suggesting that glycated albumin may play a role in the development of diabetic heart disease [9].

The relationship between AGEs and cardiovascular diseases is well known [10]. Elevated levels of AGEs were first associated with diabetes, where it was thought that AGEs formation was exclusively the result of increased blood sugar concentrations [11]. However, recent studies have extended this view and have shown that AGEs accumulation occurs also in pathological situations such as cardiac dysfunction, and renal failure, independent of diabetes [12–15].

Further, through decreased compliance of the heart and the vasculature, AGE accumulation is considered to be related to the onset and progression of heart failure (HF) [14,16].

However, the possible effects of early glycation products, such as the Amadori product, in the cardiovascular system have been less studied than the effects of the irreversible AGEs.

In this study we analyzed the levels of the Amadori product glycated-albumin (GA) in non-diabetic patients with HF and the effects of this modified protein on cardiomyocytes *in vitro*.

2. Materials and methods

2.1. Study population

Plasma samples were obtained from a subset of healthy subjects (controls) and HF patients matched according to their age, sex, and clinical characteristics, from a previously enrolled population [17]. The study was approved by the Ethical Committee European Institute of Oncology and Monzino Cardiologic Center (registration number R205-CCFM S208/412) [17]. All patients belong to a cohort of HF patients regularly followed at our HF Unit and underwent our standard HF assessment which included full clinical evaluation, standard laboratory tests, echocardiography, spirometry, and alveolar capillary diffusion, as well as cardiopulmonary exercise test. All patients had severe HF, being in New York Heart Association (NYHA) class III and IV, but were in stable clinical conditions. Patients with an established diagnosis of diabetes mellitus or under diabetes treatment were excluded. A detailed summary of the clinical characteristics, obtained as previously described [17], is reported in Table 1.

Table 1
Clinical characteristics of subjects categorized in healthy subjects, HF patients (NYHA class III), and HF patients (NYHA class IV).

	Healthy subjects (n = 10)	HF patients NYHA III (n = 7)	HF patients NYHA IV (n = 7)
Age	56.27 ± 4.69	67 ± 12.14	67.43 ± 6.24
Gender (m/f)	7/3	5/2	6/1
Hypertension	0/10	5/7	5/7
Dyslipidemia	0/10	4/7	4/7
Smoke	1/10	1/7	3/7
BMI	25.66 ± 3.42	26.68 ± 3.38	27.11 ± 4.81
Glycemia (mg/dL)	102.4 ± 12.76	105 ± 12.39	120.2 ± 12.01
GA (%)	6.53 ± 0.54	7.38 ± 1.47	8.13 ± 0.77
EF (%)	–	39.9 ± 6.57	26.86 ± 11.31
BNP (pg/mL)	–	265.14 ± 310.15	967.8 ± 668.6
DLCO (% predicted)	94.21 ± 21.06	72.09 ± 17.43	65.87 ± 12.21
VO_2 peak/Kg (mL/min/Kg)	34.58 ± 8.46	15.39 ± 8.95	11.05 ± 2.09

Data are expressed as mean ± SD. BMI, body mass index; GA, glycated human serum albumin; EF, ejection fraction; BNP, Brain natriuretic peptide; DLCO, carbon monoxide lung diffusion; VO_2, oxygen consumption; m, male; f, female.

2.2. Quantitation of glycated albumin (GA) by mass spectrometry

The relative composition of albumin isoforms in human plasma samples was evaluated, as previously described [18], by direct infusion using the Xevo TQS micro triple quadrupole mass spectrometer coupled with the M-Class UPLC system (Waters Corporation, Milford, USA). Briefly, centrifuged plasma samples at 3000 × *g* for 10 min at 4 °C were diluted 200 folds in 50% ACN containing 0.1% FA. After centrifugation at 14 000 × *g* for 10 min at 4 °C, 5 µl were injected at 5 µl/min and the spectra were acquired for 6 min with the following parameters: positive ESI mode; mass range 1100–1350 *m/z*; capillary voltage, 3 kV; cone, 90 V; desolvation temperature 350 °C; source temperature 150 °C. Data processing for deconvolution was performed with the MaxEnt1 function on the Masslynx software (Waters Corporation, Milford, USA). Mercaptoalbumin (native HSA) and GA (+160 ± 2 Da) were detected and their intensities were used to calculate the relative abundances as previously described [18] and detailed in Supplementary information.

2.3. Carboxymethyl lysine assay

Plasma levels of carboxymethyl lysine (CML) were measured with a commercially available ELISA kit (Biosite, Taby, Sweden) according to the manufacturer's instruction.

2.4. Cell culture and treatment

The HL-1 cardiomyocytes, a kind gift of Prof. W.C. Claycomb, (LSU Health Sciences Center, New Orleans, LA, USA), were cultured in complete Claycomb medium supplemented with 10% FBS (Sigma-Aldrich, Milan, Italy), 2 mmol/L L-glutamine (Thermo Fisher Scientific, Milan, Italy), and 100 µmol/L norepinephrine (Sigma-Aldrich, Milan, Italy) according to Prof. Claycomb's instructions [19]. HL-1 cells (1×10^5) were seeded onto a 6-well plate and were grown for 48 h in complete media. Before stimulation, cells were washed with PBS and then were incubated with vehicle (control cells), GA (A8301, Sigma, Milan, Italy, at 100 or 250 µg/mL corresponding to ~1.5 µmol/L or ~3.7 µmol/L, respectively), and non-glycated recombinant albumin (HSA, A9731, Sigma, Milan, Italy, at 250 µg/mL corresponding to ~3.7 µmol/L) for 8 or 16 h in Claycomb serum free medium. For secretome analysis, the treatment of the cells for 8 h and 16 h with vehicle or human albumin (GA or non-glycated) was prolonged for additional 24 h after changing the medium with serum- and phenol-free medium

[20].

2.5. MTT assay

The methylthiazolyldiphenyl-tetrazolium bromide (MTT) assay was based on the protocol first described by Mosmann [21]. Briefly, after treatment for 16 h with GA (100–250 μg/mL) or vehicle in Claycomb serum-free media as specified above, the cells were washed with PBS and incubated in serum-free and phenol-free medium for 24 h. Afterward, cells were incubated for 30 min at 37 °C with 0.1 mg/mL of MTT (Sigma-Aldrich, Milan, Italy), dissolved in serum- and phenol-free medium. At the end of the incubation, cells were dissolved in DMSO. Absorbance was recorded at 550 nm using the microplate spectrophotometer system (Mithras LB940, Berthold Technologies, Bad Wildbad, Germany). Data are expressed as absorbance values/μg of proteins.

2.6. Cell death analysis

Cytoplasmic histone-complexed DNA fragments (mono- and oligonucleosomes) were quantified as described [22] by using a one-step sandwich immunoassay (Cell death detection ELISA, Roche Diagnostics, Mannheim, Germany), according to the manufacturer's instructions. The data are expressed as absorbance at 405 nm (reference wavelength 490 nm)/μg of proteins.

2.7. Label-free mass spectrometry analysis

Secretome samples for proteomic analysis were desalted, concentrated and digested as previously described [20] with minor variations. Briefly, the cell culture media from each condition were collected and cell debris was removed by centrifugation. Then, samples were dialyzed at 4 °C using a 3500 molecular weight cut-off dialysis tubing (Spectrum Laboratories, Rancho Dominguez, CA, USA) against 5 mmol/L NH_4HCO_3 containing 0.01% EDTA, followed by dialysis against water. After lyophilization, the secreted protein pellets were dissolved in 25 mmol/L NH_4HCO_3 containing 0.1% RapiGest (Waters Corporation, Milford, MA, USA), sonicated, and centrifuged at 13 000 × *g* for 10 min. Samples (25 μg of protein) were then incubated 15 min at 80 °C and reduced with 5 mmol/L DTT at 60 °C for 15 min, followed by carbamidomethylation with 10 mmol/L iodoacetamide for 30 min at room temperature in the darkness. Then, 2 μg of sequencing grade trypsin (Promega, Milan, Italy) were added to each sample and incubated overnight at 37 °C. After digestion, 2% TFA was added to hydrolyze RapiGest and inactivate trypsin. Tryptic peptides were used for label-free mass spectrometry analysis. Label-free mass spectrometry analysis, LC-MS^E, was performed on a hybrid quadrupole-time of flight mass spectrometer coupled with a nanoUPLC system and equipped with a Trizaic source, as previously detailed [20,23].

2.8. Gene ontology analysis

Data were analyzed with the Search Tool for the Retrieval of Interacting Genes/Proteins (STRING 10.5) database [24] as previously described [25], to identify enriched gene ontology (GO) terms in the biological process, molecular function or cellular component categories.

2.9. Intracellular reactive oxygen species (ROS) formation

Generation of intracellular ROS was measured by the oxidative-sensitive fluorescent probe 2′,7′-dichlorofluorescein diacetate (DCF-DA). HL-1 cells were grown in complete media for two days on 96 black-wall clear bottom plates followed by 24 h of starvation in serum-free and phenol-free media. Cells were incubated with 10 μmol/L DCFH-DA (Sigma-Aldrich, Milan, Italy) in serum-free and phenol-free media for 1 h at 37 °C in the presence of 100 μmol/L ascorbic acid. At the end of the incubation, cells were washed in PBS and exposed to GA 250 μg/mL, HSA 250 μg/mL or vehicle for the indicated time. The production of ROS was measured by the intensity of DCF emission at 525 nm (excitation 485 nm), in a multifunctional microplate reader Tecan Infinite 200 PRO (TECAN, Milan, Italy). Results are expressed as absolute fluorescence (arbitrary units) of DCF after subtracting blank readings from all measurements.

2.10. Western blotting

Cell monolayers were harvested in Laemmli buffer (2% SDS, 10% glycerol and 62.5 mmol/L Tris, pH 6.8) containing a protease inhibitor cocktail (Sigma-Aldrich, Milan, Italy). Cell protein content was measured using the DC Protein Assay (Biorad Laboratories, Milan, Italy). Equal amounts of proteins (specifically 35 μg for the detection of HNE-adducts, 15 μg for the detection of carbonylated proteins, and 10 μg for the detection of HSP90 beta), from each condition, were separated on 12% SDS-polyacrylamide gel under reducing conditions in running buffer (25 mmol/L Tris, 3.5 mmol/L SDS, 192 mmol/L glycine) and transferred to nitrocellulose membranes in Transfer buffer with SDS (25 mmol/L Tris, 192 mmol/L glycine, 20% methanol, and 0.02% SDS) as previously described [26]. Transferred proteins were stained with MEMCode staining kit (Thermo Fisher Scientific, Milan, Italy) for loading control. The membranes were incubated with primary antibodies against 4-HNE-adducts (1:3000, Abcam, Cambridge, UK) or HSP90 beta (1:5000, Thermo Fisher Scientific, Milan, Italy), and subsequently with anti-rabbit horseradish peroxidase-conjugated secondary antibody (1:5000, Bio-Rad, Milan, Italy).

For the detection of carbonylated proteins, lyophilized pellets were suspended in 6% SDS and extracted proteins were derivatized with 20 mmol/L DNPH (in TFA 20%) for 15 min at room temperature. The DNPH-derivatized samples were then neutralized with 2 mol/L Trizma buffer containing 30% glycerol and 10% 2-β-mercaptoethanol, and the proteins were separated by SDS-PAGE and blotted to nitrocellulose membranes. Immunodetection was carried out using biotinylated anti-DNP antibody (1:5000, Invitrogen, Milan, Italy) and conjugated avidin-HRP (1:1000, Biorad, Milan, Italy) [27].

The bands were visualized by means of enhanced chemiluminescence (GE Healthcare, Milan, Italy) and analyzed with the QuantityOne software (Bio-Rad Laboratories, Milan, Italy) for densitometric analysis including normalization for total protein loading.

2.11. RNA extraction and real-time reverse transcription polymerase chain reaction (RT-PCR)

Total cellular RNA was extracted using the Total RNA purification plus kit (Norgen BioTek, Ontario, Canada) and reverse transcribed at 42 °C for 50 min, and at 70 °C for 15 min (Bio-Rad Laboratories, Milan, Italy). For 1 μg of total cellular RNA, we used 200 units of reverse transcriptase (RT; SuperScript III, Invitrogen, Life Technologies, Monza, Italy), 3 μg random hexamer primers, 1 mmol/L dNTPs, and 40 units Rnase inhibitor.

Real-time quantitative PCR (qRT-PCR) was carried out to detect Nrf2, IL-6, TNF-α, IL-10, PGC1α, and PGC1β mRNA, with GAPDH mRNA being used for sample normalization. Primers were purchased from Integrated DNA Technologies (Leuven, Belgium) and the primer sequences were: mouse GAPDH sense 5′ CGTGCCGCCTGαAACC 3′; mouse GAPDH antisense: 5′ TGGAAGAGTGGGAGTTGCTGTTG 3′; mouse Nrf2 sense 5′ GATGCTCATGAAATTTGCCTGC 3′ and mouse Nrf2 antisense: 5′ ACAAGCTTCGGTCTGGATCCA 3′. Primers for IL-6 (QT00098875), TNF-α (QT00104006), IL-10 (QT00106169), PGC1α (QT02524242), and PGC1β (QT00125272), were purchased from Qiagen (Milan, Italy). qRT-PCR was carried out as previously described on the iCycler optical system (Bio-Rad Laboratories, Milan, Italy) [28].

2.12. Statistical analysis

Clinical data from healthy subjects (control) and HF patients were analyzed using SAS v9.4 (SAS Institute, Cary, NC, USA) and are expressed as mean ± standard deviation (SD), subdividing HF patients according to NYHA class (III vs IV). Univariate analysis was performed by ANOVA to identify statistically different variables among groups while Pearson correlation was used to identify a possible correlation between GA and clinical variables. General linear model (GLM) was used to highlight the trend of increase of GA with the gravity of the disease, both as univariate analysis and as multivariate analysis taking into consideration differences of age and presence of hypertension.

Data obtained from *in vitro* experiments were expressed as mean values ± SEM and analyzed with GraphPad Prism v5.03 using ANOVA for repeated measures, followed by Tukey's test (n = the number of individual experiments performed in duplicate or triplicate), after normality assessment by Kolmogorov-Smirnov tests. p values of < 0.05 were considered significant.

3. Results

3.1. Analysis of glycated albumin in heart failure patients

Mass spectrometry analysis of albumin in human plasma samples allowed us to calculate the fraction of GA with respect to all the albumin isoforms (Fig. 1A). Comparing the percentage of GA between healthy subjects and HF patients, subdivided according to HF severity as inferable from the NYHA class (III *vs* IV), we observed an increase of GA in the plasma of the patients with respect to the healthy subjects (6.53 ± 0.54% for healthy subjects, 7.38 ± 1.47% for HF class III, and 8.13 ± 0.77% for HF class IV, Table 1). The statistical analysis demonstrated that the percentage of GA was significantly higher in the patients' group with the higher degree of HF severity (Fig. 1B), according to a univariate ANOVA analysis ($p = 0.0075$) and GLM analysis ($p = 0.0022$). Considering that age and presence of hypertension correlate with GA and are significantly different among groups, a multivariate GLM analysis was also performed after adjustment for age and hypertension revealing a significant association of GA with HF severity ($p = 0.0391$). Of note, we detected an inverse correlation between GA and peak VO_2/Kg (Fig. 1C), a known index of oxygen consumption previously associated with HF severity [17].

Analysis of CML levels on the plasma of HF patients and controls did not reveal any significant changes (Supplementary Fig. 1), thus indicating that in our samples early glycation, not advanced glycation, was present (data not shown).

3.2. Proteomic analysis of the secretome from HL-1 treated with GA

In order to investigate the effects of GA on HL-1 cardiomyocytes, we stimulated the cells with the purified commercially available GA. To this purpose, we first characterized the glycation sites present in the purified commercially available GA and in the one isolated from plasma of HF patients by means of mass spectrometry (details are available in the Supplementary Material). Results showed that 8 out of 9 glycated residues found in the human albumin from HF patients were also present in the purified commercially available GA (Supplementary Fig. 2 and Supplementary Table S1). Additional modified residues were detected only in the purified commercially available GA, although the majority at a low relative abundance (Supplementary Table S1).

Aiming to elucidate the biological impact of GA on HL-1 cardiomyocytes, we first determined the influence of GA on cell viability and apoptosis. The cells were stimulated with GA (100 or 250 μg/mL) for 16 h and then subjected to MTT assay. As reported in Fig. 2A, cells treated with GA (250 μg/mL) exhibited a slightly decreased in proliferation (−10%, $p < 0.05$) compared to the control cells. Further, apoptosis was assessed by means of Cell Death Detection ELISA assay, which measures cytosolic histone-associated DNA fragments present in the cell lysates. Results indicated that cell apoptotic responses remained unchanged after GA treatment (Fig. 2B).

For the proteomic analysis, HL-1 cells were pre-treated for 8 h or 16 h with GA (100 or 250 μg/mL) in serum-free Claycomb medium and then incubated for 24 h, in serum-free phenol-free medium in the absence of GA, in order to collect secreted proteins without the contamination of the exogenously added GA. Then, employing a label-free mass spectrometry based method (LC-MS^E) [20], we compared the secretome after GA treatment at the two different time points (8 h and 16 h) and identified those proteins that were differently abundant.

This approach allowed us to identify a total of 216 and 246 proteins in cells incubated for 8 h or 16 h, respectively, as reported in Supplementary Tables S2 and S3. After treatment with GA for 8 h, eight proteins were less abundant after treatment with 250 μg/mL GA, and only one was released at higher extent (Table 2). At 16 h, six proteins were more abundant after treatment with 250 μg/mL GA, while eight were more abundant in the secretome of control cells (Table 3).

The lists of differentially abundant proteins were analyzed with STRING for evaluation of protein-protein interactions and gene ontology analysis in order to find out the enriched biological processes. As shown in Fig. 3, considering only the proteins that were modulated after 8 h, no significantly enriched biological process was detected, while among proteins modulated after 16 h of treatment some biological processes, including response to organic substance and response to stress, were significantly enriched.

Of note, three proteins (Heat shock protein HSP90 beta, Nucleolin and Heat shock protein HSP90 alpha) belonging to these biological processes were commonly modulated at 8 h and 16 h, as shown in the Venn diagram in Fig. 4.

Thus, in order to verify the proteomic results, we confirmed by immunoblotting that treatment with GA significantly reduced the release of Heat shock protein HSP90 beta (Fig. 5). This modulation was not observed when cells were stimulated with non-glycated HSA (250 μg/mL) (Supplementary Fig. 3A).

3.3. Effects of GA on protein oxidation and lipoxidation

In view of the statistically significant enrichment of the GO term related to response to stress, we next assessed the capacity of GA to cause oxidative damage.

Exposure of HL-1 cells to GA resulted in the rapid intracellular generation of ROS, assessed by DCF fluorescence (Fig. 6). When cells were in presence of non-glycated HSA no increase in ROS levels was observed (Supplementary Fig. 3B).

Subsequently, we investigated whether GA mediated downstream oxidative damage to proteins. We evaluated, by means of western blot, intracellular 4-hydroxynonenal-protein adducts and carbonylated protein levels, both biomarkers of protein oxidation and lipoxidation. Levels of adducted proteins with 4-hydroxynonenal (4-HNE) after 8 h and 16 h of cell treatment with GA are shown in Fig. 7A and C, and Supplementary Figs. 4B and 4C. Densitometric analysis revealed that 4-HNE-protein adduct levels increased dose-dependently at 8 h, being statistically significant when the cells were incubated with GA (250 μg/mL) (Fig. 7B). 4-HNE-protein adducts formation after 16 h of cell treatment with GA did not change with respect to the control cells (Fig. 7D).

Carbonylated protein levels of cells treated with GA were detected after DNPH derivatization of the carbonyl groups using an anti-DNP antibody (Fig. 8A and C, Supplementary Figs. 4D and 4E). Densitometric analysis unveiled that cells treated with GA showed a significant increase in protein carbonylation in comparison with control cells at 16 h (Fig. 8B and D). Cells treatment with non-glycated HSA (250 μg/mL) did not show differences in the levels of carbonylated proteins with respect to the control cells (Supplementary Figs. 3C and 3D).

Additionally, it was also investigated if GA could modulate mRNA

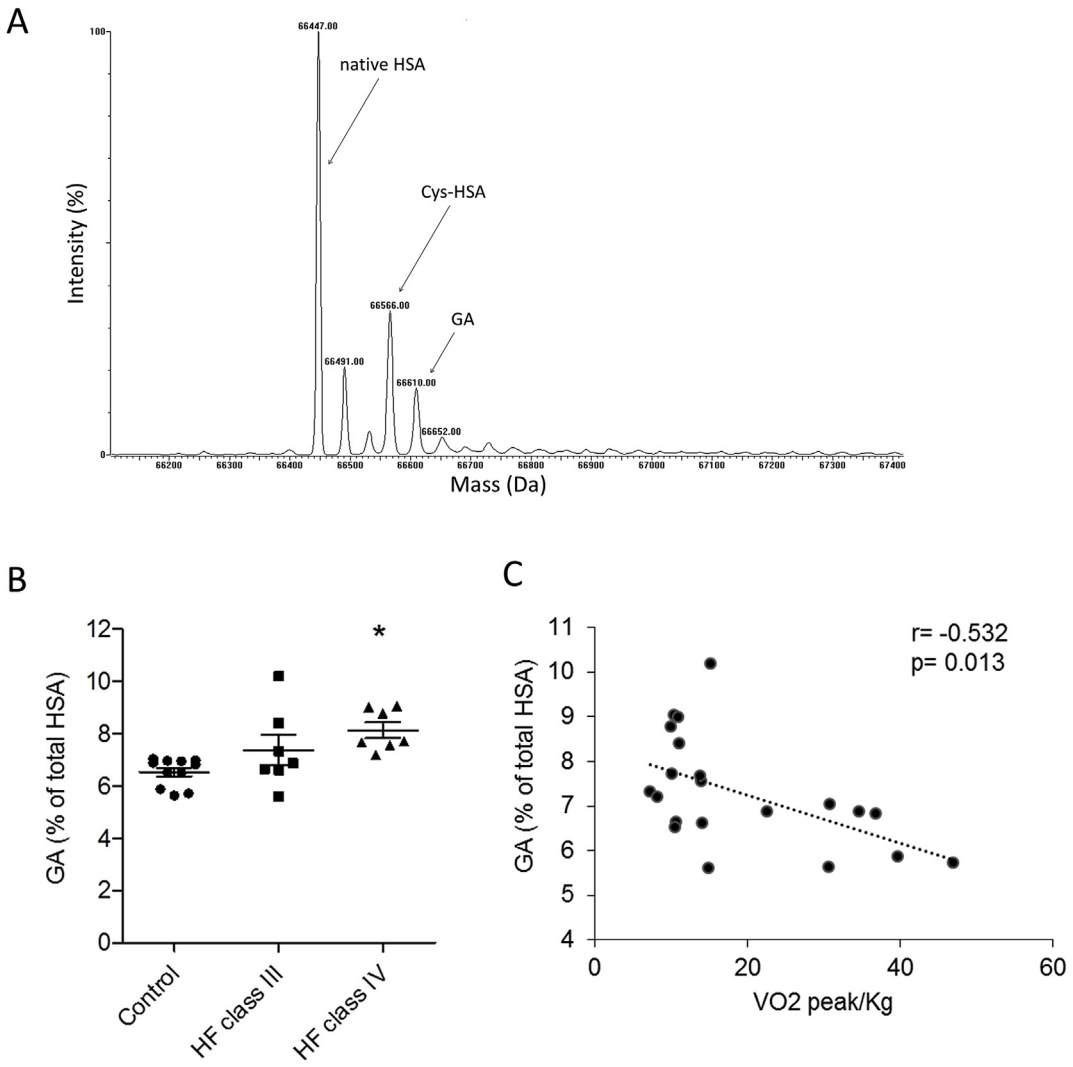

Fig. 1. Glycated albumin (GA) in heart failure patients. A) Representative deconvoluted ESI-MS spectrum of albumin from plasma of a HF patient. Arrows indicate the mercaptoalbumin (native HSA), the cysteinylated (Cys-HSA), and the glycated (GA) albumin isoforms characterized by a mass shift of 119 ± 2 and 162 ± 2 Da with respect to the native HSA, respectively. ESI-MS spectra were acquired in positive ion mode and setting a scan range of *m/z* 1100–1350. B) The percentage of GA with respect to the total amount of albumin has been analyzed by mass spectrometry in healthy subjects (controls) and HF patients divided in NYHA class III and class IV. Observed GA percentage values were 6.53 ± 0.54%, 7.38 ± 1.47%, and 8.13 ± 0.77% for healthy subjects, HF class III, and HF class IV, respectively. Values are represented as mean ± SEM. *p < 0.05 *vs* controls. C) Correlation between the percentage of GA and peak VO_2/Kg. HSA, human serum albumin.

expression levels of nuclear factor (erythroid-derived 2)-like 2 (Nrf2). Our results showed a significant increase of Nrf2 mRNA when the cells were treated with 250 µg/mL GA, either after 8 h and 16 h (Fig. 9). This effect was not observed when the cells were treated with non-glycated HSA (Supplementary Fig. 3E).

3.4. Effects of GA on inflammation and mitochondrial biogenesis mediators

Further, our results highlighted a significantly enhanced IL-6 mRNA production only after 8 h of treatment with GA (100 or 250 µg/mL) (Fig. 10A and E). The levels of IL-6 mRNA were not significantly

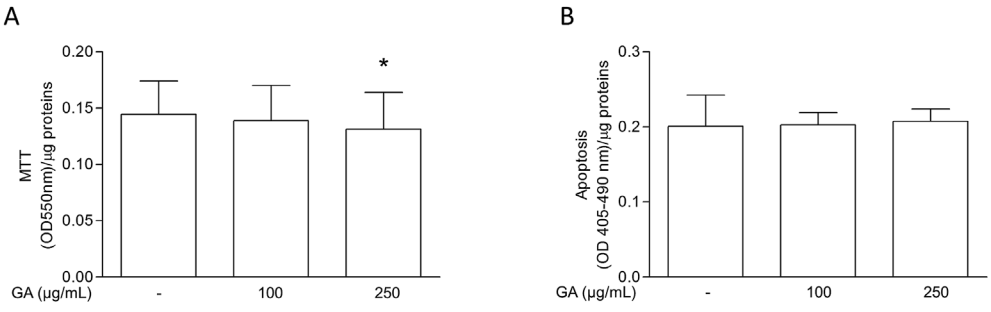

Fig. 2. Effects of GA on HL-1 cell proliferation and apoptosis. A) HL-1 cells were stimulated with GA (100 or 250 µg/mL) for 16 h and then cultured in serum-free phenol-free medium for additional 24 h. Cell proliferation assay was performed employing the MTT colorimetric method. Data are expressed as the means ± SEM of absorbance values/µg of proteins from 3 independent experiments. *p < 0.05 compared to control cells. B) Analysis of apoptosis. Cells were stimulated with GA for 16 h. Cell lysates were collected to measure apoptosis after 24 h of incubation in serum-free and phenol-free by means of Cell Death Detection ELISA Plus assay. Data are expressed as the means ± SEM of absorbance values/µg of proteins from 3 independent experiments.

Table 2
List of differentially abundant proteins in the secretome of HL-1 cells treated with GA for 8 h identified by LC-MS^E and analyzed with Progenesis QIP.

Accession	Description	Peptide count/Unique peptides	Score[a]	Anova (p)	Max fold change	Highest mean condition	Lowest mean condition
P14869	60S acidic ribosomal protein P0	6/3	32.6	2.67E-06	1.422	CTRL	250
P09405	Nucleolin	7/5	38.4	1.55E-13	1.413	CTRL	250
P26350	Prothymosin alpha	3/2	25.4	2.86E-05	1.397	CTRL	250
P14131	40S ribosomal protein S16	4/3	26.0	0.000763	1.312	CTRL	250
P11499	Heat shock protein HSP90 beta	37/18	266.4	5.77E-09	1.263	CTRL	250
P02301	Histone H3.3C	14/10	79.3	0.243 836	1.239	CTRL	250
Q03265	ATP synthase subunit alpha, mitochondrial	13/6	70.4	6.63E-06	1.236	CTRL	250
P07901	Heat shock protein HSP90 alpha	25/7	160.9	1.73E-06	1.205	CTRL	250
P68037	Ubiquitin-conjugating enzyme E2 L3	3/3	19.6	0.077 822	1.258	250	CTRL

[a] Confidence score for protein identification from Progenesis QIP; CTRL, control; 250, GA concentration (μg/mL).

Table 3
List of differentially abundant proteins in the secretome of HL-1 cells treated with GA for 16 h identified by LC-MS^E and analyzed with Progenesis QIP.

Accession	Description	Peptide count/Unique peptides	Score[a]	Anova (p)	Max fold change	Highest mean condition	Lowest mean condition
P51881	ADP/ATP translocase 2	5/2	30.1	0.0298	2.029	CTRL	100
P09405	Nucleolin	11/5	65.6	0.0049	1.764	CTRL	250
P11499	Heat shock protein HSP90 beta	37/13	297.9	0.0006	1.678	CTRL	250
P63158	High mobility group protein B1	4/2	21.7	0.0233	1.511	CTRL	250
P08113	Endoplasmin	11/2	57.6	0.0044	1.403	CTRL	250
P07901	Heat shock protein HSP90 alpha	31/10	218.6	0.0500	1.301	CTRL	250
Q9CS84	Neurexin-1	2/2	8.9	0.0035	1.247	CTRL	250
P14211	Calreticulin	11/6	89.2	0.0399	1.222	CTRL	250
O89086	RNA-binding protein 3	5/2	39.6	0.0001	1.467	250	CTRL
Q8CGC7	Bifunctional glutamate/proline–tRNA ligase	18/8	96.4	0.0013	1.336	250	CTRL
Q7TMK9	Heterogeneous nuclear ribonucleoprotein Q	9/4	48.1	0.0017	1.243	250	CTRL
P05201	Aspartate aminotransferase, cytoplasmic	25/17	196.7	0.0000	1.234	250	CTRL
P63017	Heat shock cognate 71 kDa protein	44/20	449.6	0.0007	1.223	250	CTRL
Q99JF5	Diphosphomevalonate decarboxylase	2/2	10.9	0.0425	1.204	250	CTRL

[a] Confidence score for protein identification from Progenesis QIP; CTRL, control; 100 or 250, GA concentration.

affected when the cells were treated for 8 h with non-glycated HSA (250 μg/mL) (Supplementary Fig. 3F). Additionally, a significant increase of TNF-α mRNA levels was observed in cells treated with GA (250 μg/mL), but not with non-glycated HSA, for 8 h (Fig. 10B and Supplementary Fig. 3G). The anti-inflammatory cytokine interleukin-10 (IL-10) mRNA was not detectable even after stimulation with GA (data not shown).

We next investigated the effects of GA on the expression of peroxisome proliferator-activated receptor gamma coactivator 1-alpha and beta (PGC1α and PGC1β respectively), two genes involved in the mitochondrial biogenesis. As regards PGC1α, no significant modulations were observed either after 8 h or 16 h of treatment (Fig. 10C and F). By the contrary, PGC1β mRNA levels raised after 8 h of treatment with GA (Fig. 10D and G).

4. Discussion

In this study, we found an increased amount of glycated albumin, measured by quantitative mass spectrometry, in the plasma of HF patients, and we took advantage of a proteomics-based approach to assess the effects of GA in *in vitro* cultured cardiomyocytes. Further, a functional interpretation of the identified proteins, obtained by searching the Gene Ontology (GO) annotations for over-represented terms, revealed that GA is a potential mediator of the response to stress.

Among proteins decreased after GA treatment, we found HSP90, one of the most abundant cellular HSPs that contributes intracellularly to

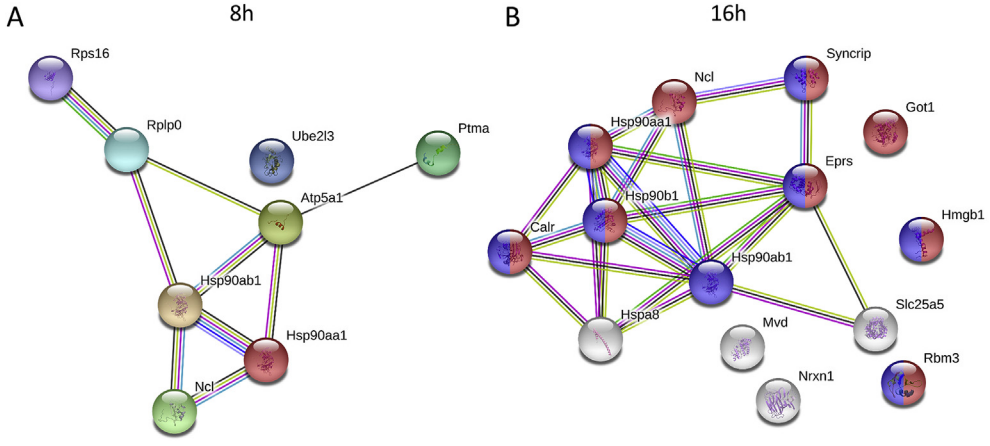

Fig. 3. Gene ontology analysis of secreted proteins modulated by GA visualized with STRING. A) Protein network obtained with proteins modulated after 8 h of treatment with GA. B) Protein network obtained with proteins modulated after 16 h of treatment with GA in which enriched biological processes are highlighted. In B, proteins associated with the GO term response to stress are colored in blue (p = 0.0229), while proteins associated with the response to organic substances are colored in red (p = 0.000222).

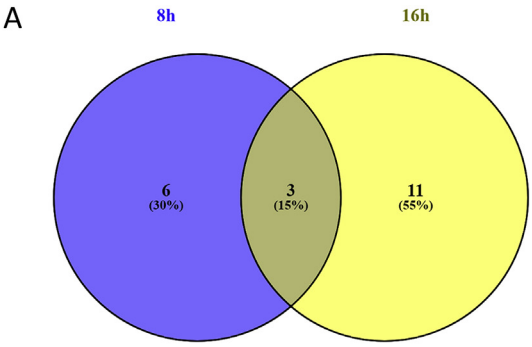

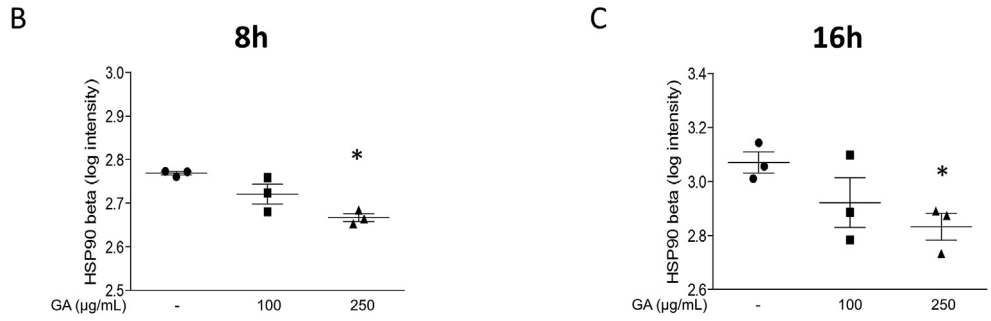

Fig. 4. Proteomic analysis of HL-1 secretome after treatment with GA. A) Venn diagram of the modulated proteins after 8 h and 16 h of incubation with GA. B–C) Graphical representation of the intensity of one of the 3 proteins that are modulated at both time points, Heat shock protein 90 beta (HSP90 beta), obtained by label free MS analysis after treatment with GA for 8 h (B) or 16 h (C). *p value $<$ 0.05 *vs* control cells.

cell survival and protection by regulating the folding and stability of a wide range of key cellular proteins, including survival and apoptotic factors [29]. HSP90 efficiently ameliorates myocardial IR-induce myocardial dysfunction in ischemic condition [30] and exerts an anti-apoptotic effect on cardiomyocytes subjected to hypoxia [31], whereas the inhibition of HSP90 markedly diminishes the protective effects of hypoxic pre-conditioning against prolonged hypoxia/reoxygenation-induced injury in H9C2 cardiac cells [32]. On the other hand, extracellular HSP90 predisposes vascular smooth muscle cells to a pro-inflammatory phenotype by IL-8 elevation in the stressed vasculature [33]. Additionally, the association of extracellular HSP90 with transforming growth factor β receptor I (TGCβRI) at the surface of cardiac fibroblast plasma membrane is critical in collagen production during fibrotic processes [34].

The role of HSPs in the glycated bovine serum albumin mediated effects has been previously observed in cultured β-cells in which a HSP60-correlated signaling pathway was hypothesized to contribute to the AGEs-RAGE axis-induced β-cell hypertrophy and dysfunction under diabetic hyperglycemia [35].

Nevertheless, there is still limited information with respect to the HSPs extracellular role on cardiomyocytes and their relationship with the pathogenesis of HF.

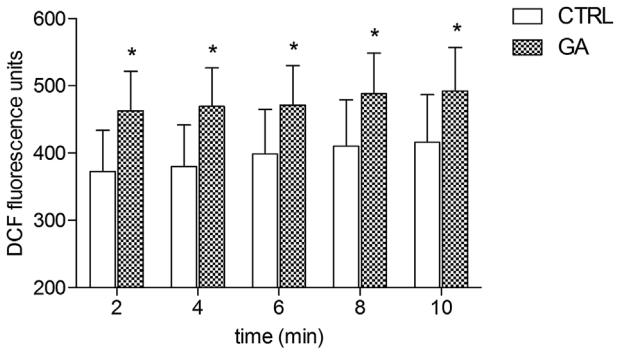

Fig. 6. Intracellular generation of reactive oxygen species (ROS) mediated by GA. HL-1 cells were loaded with 10 μmol/L DCF-DA and stimulated with GA (250 μg/mL) for different times. Data shown represent the averages of three independent experiments (mean ± SEM). *p $<$ 0.05 *vs* untreated cells.

Moreover, we found that exposure of cardiomyocytes to GA resulted in oxidative modifications, in terms of carbonylation or lipoxidation adducts, of a multitude of cellular proteins. We indeed observed that GA significantly enhances ROS production, which is in agreement with

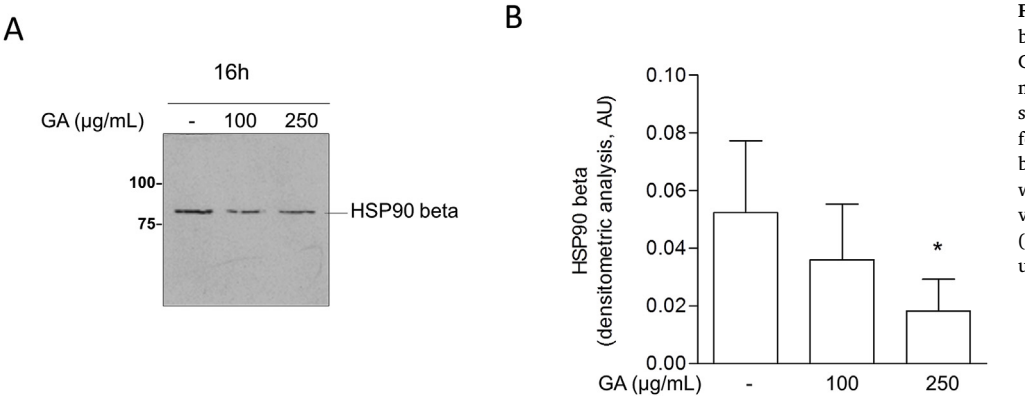

Fig. 5. Immunoblotting analysis of HSP90 beta in HL-1 secretome after treatment with GA. A) Representative image of immunoblotting analysis of HSP90 beta in the secretome from HL-1 cells treated with GA for 16 h. B) Densitometric analysis of HSP90 beta from 3 independent experiments. Data were normalized for total protein loading visualized with the MEMcode staining (Supplementary Fig. 4A). *p $<$ 0.05 *vs* untreated cells.

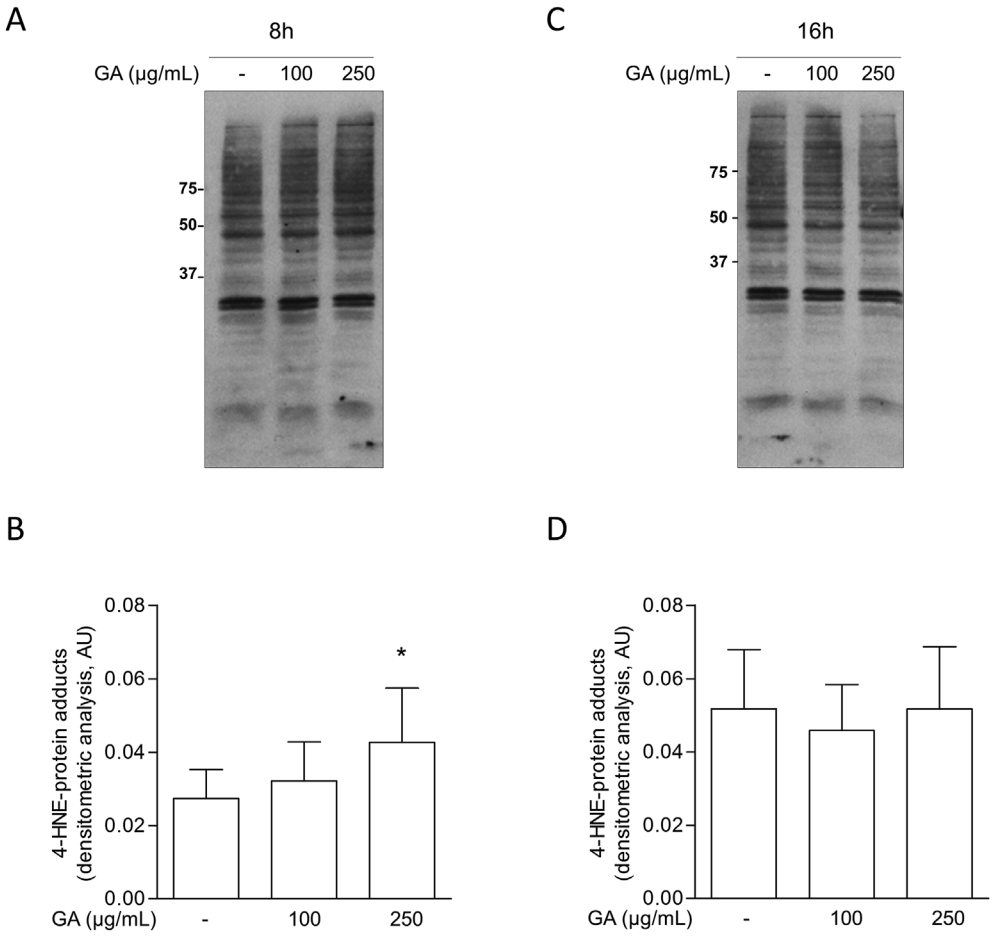

Fig. 7. Effect of GA on protein lipoxidation. Immunoblotting were performed using antibody against 4-HNE for the detection of 4-HNE-protein adducts. A) Representative western blot showing 4-HNE-protein adducts after treatment with 100 or 250 μg/mL GA for 8 h, and C) for 16 h. B) Densitometric analysis of western blots corresponding to 4-HNE immunoreactivity after 8 h and D) 16 h of treatment with GA. Data were normalized for total protein loading visualized with the MEMcode staining. Values are representative of 8 experiments and are expressed as mean ± SEM. *p < 0.05 compared to control cells.

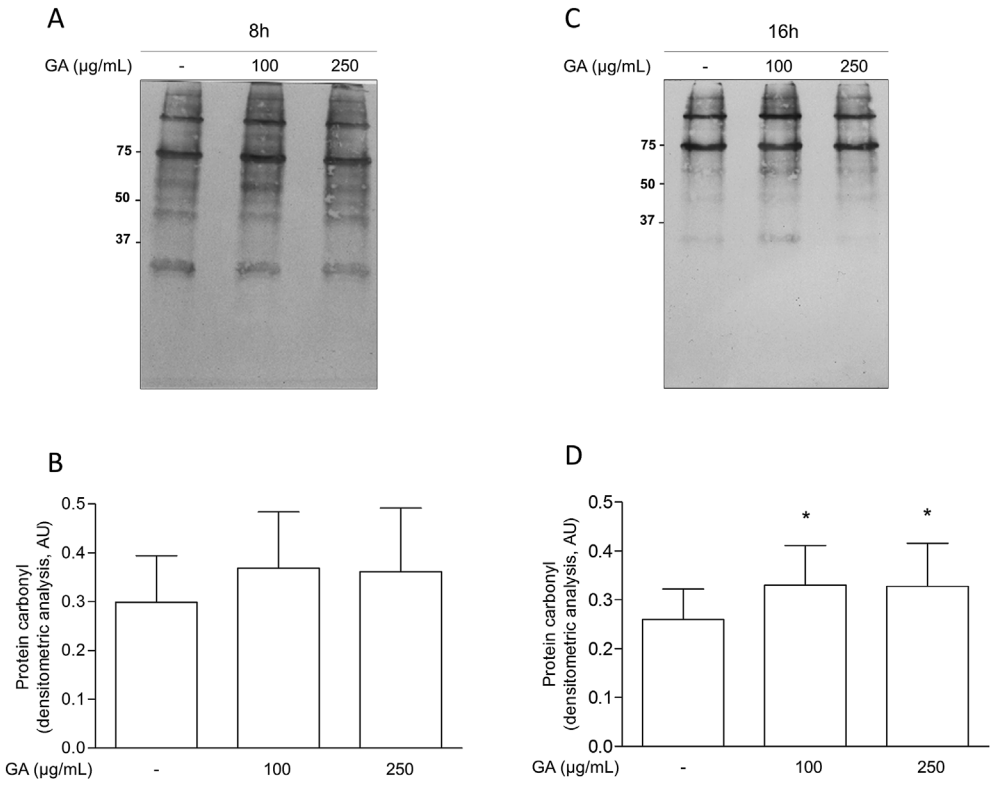

Fig. 8. Effect of GA on protein oxidation. Immunoblotting were performed using antibody against DNP for the detection of carbonylated proteins. A) Representative western blot showing carbonylated protein signal after treatment with 100 or 250 μg/mL GA for 8 h and C) 16 h. B) Densitometric analysis relative to carbonylated protein levels after 8 h and D) 16 h of incubation with GA. Values are representative of at least 8 experiments and are expressed as mean ± SEM. *p < 0.05 compared to control cells.

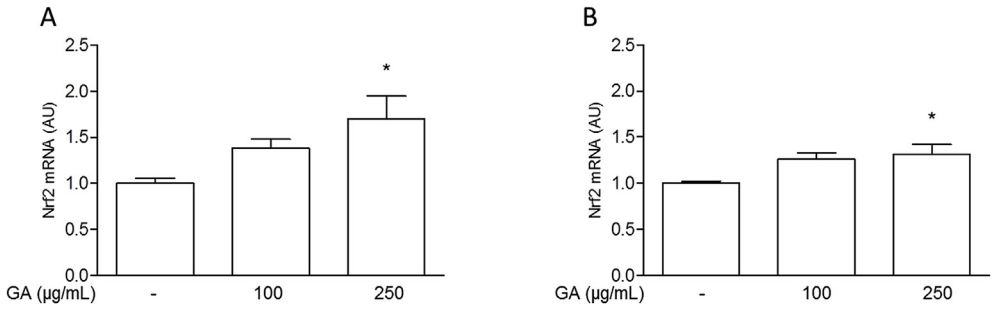

Fig. 9. Effect of GA on Nrf2 at mRNA level. Transcript expression levels analyzed by RT-qPCR were measured after A) 8 h and B) 16 h of treatment with 100 or 250 μg/mL GA. Gene expression was normalized relative to the expression of the glyceraldehyde-3-phosphate dehydrogenase (GAPDH). Results are based on 3 independent analysis and data are presented as mean ± SEM. *p < 0.05 *vs* control.

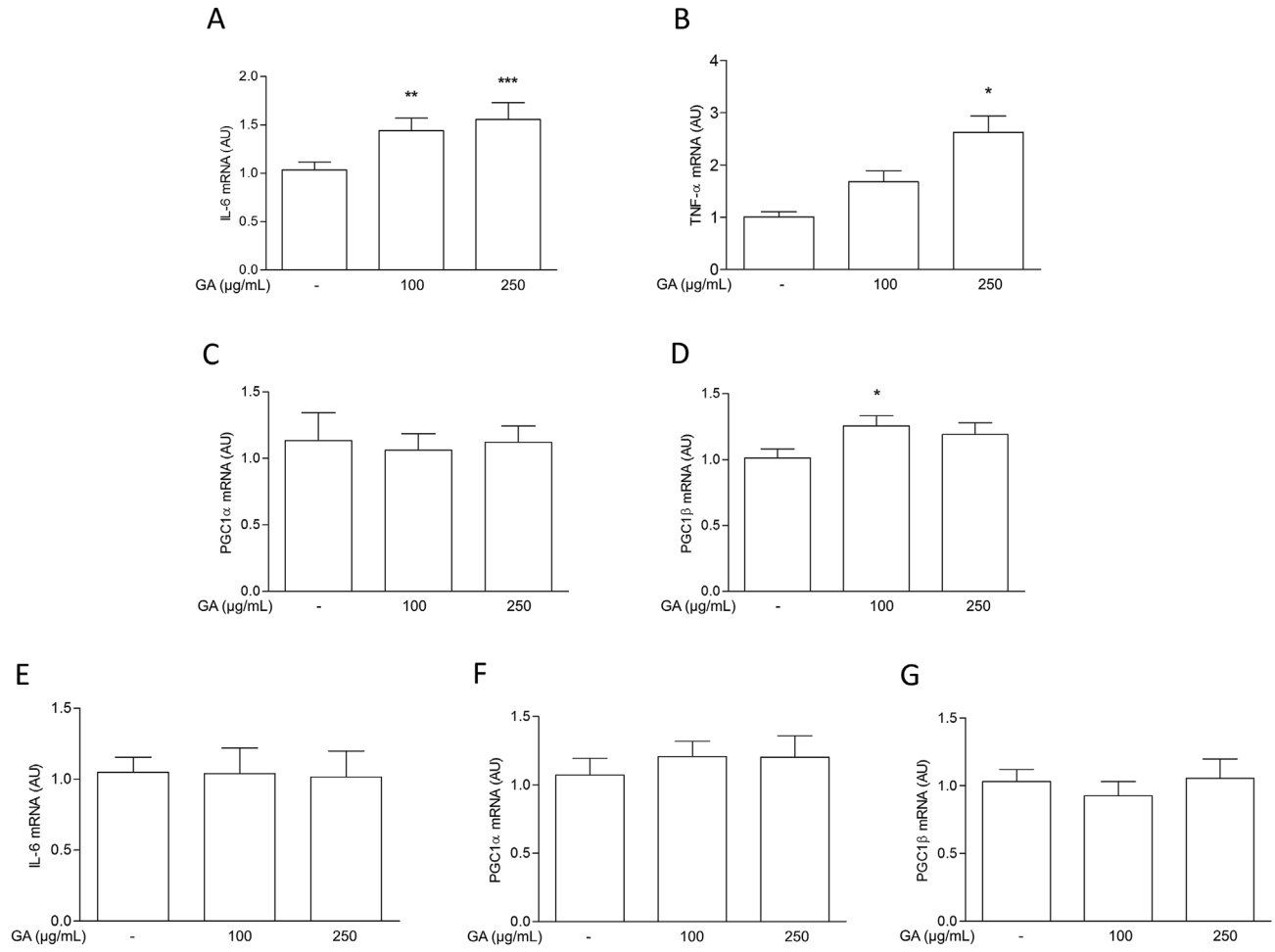

Fig. 10. Effect of GA on the mRNA levels of IL-6, TNF-α, PGC1α, and PGC1β. mRNA levels of A) IL-6, B) TNF-α, C) PGC1α, and D) PGC1β after 8 h of treatment with 100 or 250 μg/mL of GA were analyzed by RT-qPCR. mRNA levels of E) IL-6, F) PGC1α, and G) PGC1β were evaluated after 16 h or treatment with 100 or 250 μg/mL GA. Gene expression was normalized relative to the expression of the glyceraldehyde-3-phosphate dehydrogenase (GAPDH). Results are based on 10 independent experiments for IL-6, PGC1α, and PGC1β genes and on 3 independent experiments for TNF-α. Data are presented as mean ± SEM. *p < 0.05 *vs* control cells, **p < 0.01 *vs* control cells, ***p < 0.001 *vs* control cells.

previous works [36], and modulates the expression of Nrf2, a master transcription factor that becomes upregulated in response to oxidative stress [37]. The observed increase in protein carbonylation and 4-HNE-protein adduct formation can be a downstream effect of the oxidative stress mediated by GA, where excessive ROS may either oxidize proteins directly or modify them indirectly through the adduction of small breakdown products of lipid peroxidation such as 4-HNE [38]. The increase in the levels of 4-HNE modified proteins at 8 h, but not later, is suggestive of their removal by the proteasomal system, as reported by Griesser et al. [39].

The first evidence of a connection between GA and oxidative stress was the suppression of GA-induced cell apoptosis by antioxidants in bovine retinal pericytes [40]. In macrophages, GA activates ERK-dependent increases in TGF-β1 production, through oxidative stress and NF-κB induction [41]. An accumulation of oxidatively modified proteins, mainly structural proteins (i.e. ACTB and Annexin A2), was observed in human mature adipocytes incubated with GA [42]. Further, GA induces lipid infiltration in mice aorta independently of diabetes and of renin-angiotensin system local modulation by inducing lipid peroxidation and inflammation [43].

We also analyzed the expression levels of the transcriptional coactivator peroxisome proliferator-activated receptor γ coactivator-1 α (PGC-1α) and β (PGC-1 β), which, beyond their role as 'master regulator' of mitochondrial biogenesis, have been identified as inducer of

many antioxidant-detoxifying enzymes [44–46]. Downregulation of PGC-1α causes indeed an increase of intracellular ROS levels and carbonylated proteins and a decrease of antioxidant enzymes [47]. Additionally, mitochondrial activity and ROS scavenging in skeletal muscles of PGC-1β deficient mice can be enhanced by PGC-1β [46]. In our study we observed an early increase in the expression of PGC-1β but not of PGC-1α, suggesting that they cannot completely counteract the pro-oxidant effects of GA.

We also found that GA increased the expression of the pro-inflammatory cytokines IL-6 and TNF-α. Previous studies have indeed shown that GA upregulates several inflammatory mediators through the NF-κB and AP-1 signaling pathways in smooth muscle cells and endothelial cells [48,49]. Of interest, GA stimulates cell growth and migration in smooth muscle cells and fibroblasts [48,50], suggesting that GA may play a role in atherogenesis by inducing both inflammatory mediators in the vessel wall, as well as proliferative and migratory effects. By contrast, in cardiomyocytes GA slightly reduced cell viability thus supporting the hypothesis that GA plays a role in cardiac dysfunction [51].

In conclusion, this study shows that GA, measured by mass spectrometry, is elevated in the plasma of patients with HF, and it is highest in subjects with the most severe HF, thus expanding previous observations obtained by means of an enzymatic assay [52]. Specifically, Selvin et al. found a significant association of GA with cardiovascular outcomes (new cases of coronary heart disease, ischemic stroke, HF, and deaths), even after adjustment for traditional cardiovascular risk factors, in 11 104 participants with and without diabetes, during two decades of follow-up of in the community-based Atherosclerosis Risk in Communities (ARIC) Study.

Further, the findings that GA exerts pro-inflammatory and pro-oxidant effects on murine HL-1 cardiomyocytes, highlight a causal role in the etiopathogenesis of HF. However, some limitations need to be acknowledged. Indeed, other factors rather than only HF may contribute to increase the GA levels in this population studied. Further, due to the small sample size, we did not study patients with moderate HF or patients at high risk of HF, so that the progressive role of GA in the development of HF is still unknown, albeit the correlation between GA levels and peak VO_2 suggests it. Finally, our results could provide a mechanistic base for a possible use of the new antidiabetic drugs (DPP-4 inhibitors) in non-diabetic HF patients due to their favourable effect in reducing glycated proteins, specifically haemoglobin [53].

This study also highlights the role of mass spectrometry for the detection and quantitation of specific protein modifications, and contributes to strengthen the value of GA measurement over that of HbA1c which has important limitations: it does not change rapidly in response to changes in treatment, and a number of conditions affect the validity of the test result (eg, anemia, altered red cell lifespan, transfusion, kidney disease, liver disease, and abnormal forms of hemoglobin).

Declarations of interest

None.

Funding

This work was supported by the European Union's Horizon 2020 research and innovation programme under the Marie Sklodowska-Curie (grant agreement number 675132) and by the Italian Ministry of Health, Rome, Italy (Ricerca Corrente 2017 BIO 18, ID 2631209).

Aknowledgement

The Authors thank Prof William Claycomb, (LSU Health Sciences Center, New Orleans, LA, USA) for the kind gift of the HL-1 cells; Dr Alice Bonomi (Centro Cardiologico Monzino, IRCCS, Milano, Italy) for her excellent assistance in the statistical analysis; and Dr Alessandra Altomare (Department of Pharmaceutical Sciences, Università degli Studi di Milano, Milano, Italy) for the analysis of albumin modifications.

Appendix A. Supplementary data

Supplementary data to this article can be found online at https://doi.org/10.1016/j.freeradbiomed.2019.06.023.

References

[1] R. Ferrer, X. Mateu, E. Maseda, J.C. Yebenes, C. Aldecoa, C. De Haro, J.C. Ruiz-Rodriguez, J. Garnacho-Montero, Non-oncotic properties of albumin. A multidisciplinary vision about the implications for critically ill patients, Expert Rev. Clin. Pharmacol. 11 (2) (2018) 125–137, https://doi.org/10.1080/17512433.2018.1412827.

[2] F. Zsila, Subdomain IB is the third major drug binding region of human serum albumin: toward the three-sites model, Mol. Pharm. 10 (5) (2013) 1668–1682, https://doi.org/10.1021/mp400027q.

[3] P. Rondeau, E. Bourdon, The glycation of albumin: structural and functional impacts, Biochimie 93 (4) (2011) 645–658, https://doi.org/10.1016/j.biochi.2010.12.003.

[4] M.P. Cohen, Clinical, pathophysiological and structure/function consequences of modification of albumin by Amadori-glucose adducts, Biochim. Biophys. Acta 1830 (12) (2013) 5480–5485, https://doi.org/10.1016/j.bbagen.2013.04.024.

[5] I. Soaita, W. Yin, D.A. Rubenstein, Glycated albumin modifies platelet adhesion and aggregation responses, Platelets 28 (7) (2017) 682–690, https://doi.org/10.1080/09537104.2016.1260703.

[6] B.K. Rodino-Janeiro, B. Paradela-Dobarro, S. Raposeiras-Roubin, M. Gonzalez-Peteiro, J.R. Gonzalez-Juanatey, E. Alvarez, Glycated human serum albumin induces NF-kappaB activation and endothelial nitric oxide synthase uncoupling in human umbilical vein endothelial cells, J. Diabet. Complicat. 29 (8) (2015) 984–992, https://doi.org/10.1016/j.jdiacomp.2015.07.016.

[7] J. Patche, D. Girard, A. Catan, F. Boyer, A. Dobi, C. Planesse, N. Diotel, A. Guerin-Dubourg, P. Baret, S.B. Bravo, B. Paradela-Dobarro, E. Alvarez, M.F. Essop, O. Meilhac, E. Bourdon, P. Rondeau, Diabetes-induced hepatic oxidative stress: a new pathogenic role for glycated albumin, Free Radic. Biol. Med. 102 (2017) 133–148, https://doi.org/10.1016/j.freeradbiomed.2016.11.026.

[8] S.A. Harrison, Liver disease in patients with diabetes mellitus, J. Clin. Gastroenterol. 40 (1) (2006) 68–76 https://doi.org/10.1097/01.mcg.0000190774.91875.d2.

[9] M. Zhang, A.L. Kho, N. Anilkumar, R. Chibber, P.J. Pagano, A.M. Shah, A.C. Cave, Glycated proteins stimulate reactive oxygen species production in cardiac myocytes: involvement of Nox2 (gp91phox)-containing NADPH oxidase, Circulation 113 (9) (2006) 1235–1243, https://doi.org/10.1161/CIRCULATIONAHA.105.581397.

[10] D. Deluyker, L. Evens, V. Bito, Advanced glycation end products (AGEs) and cardiovascular dysfunction: focus on high molecular weight AGEs, Amino Acids 49 (9) (2017) 1535–1541, https://doi.org/10.1007/s00726-017-2464-8.

[11] M. Brownlee, Advanced protein glycosylation in diabetes and aging, Annu. Rev. Med. 46 (1995) 223–234, https://doi.org/10.1146/annurev.med.46.1.223.

[12] E.D. McNair, C.R. Wells, A.M. Qureshi, R.S. Basran, C. Pearce, J. Orvold, J. Devilliers, K. Prasad, Low levels of soluble receptor for advanced glycation end products in non-ST elevation myocardial infarction patients, Int. J. Angiol. 18 (4) (2009) 187–192 https://doi.org/10.1055/s-0031-1278352.

[13] S. Willemsen, J.W. Hartog, M.R. Heiner-Fokkema, D.J. van Veldhuisen, A.A. Voors, Advanced glycation end-products, a pathophysiological pathway in the cardiorenal syndrome, Heart Fail. Rev. 17 (2) (2012) 221–228, https://doi.org/10.1007/s10741-010-9225-z.

[14] S. Willemsen, J.W. Hartog, D.J. van Veldhuisen, P. van der Meer, J.F. Roze, T. Jaarsma, C. Schalkwijk, I.C. van der Horst, H.L. Hillege, A.A. Voors, The role of advanced glycation end-products and their receptor on outcome in heart failure patients with preserved and reduced ejection fraction, Am. Heart J. 164 (5) (2012) 742–749, https://doi.org/10.1016/j.ahj.2012.07.027 e3.

[15] G. Misciagna, G. De Michele, M. Trevisan, Non enzymatic glycated proteins in the blood and cardiovascular disease, Curr. Pharmaceut. Des. 13 (36) (2007) 3688–3695 https://doi.org/10.2174/138161207783018545.

[16] J.W. Hartog, A.A. Voors, S.J. Bakker, A.J. Smit, D.J. van Veldhuisen, Advanced glycation end-products (AGEs) and heart failure: pathophysiology and clinical implications, Eur. J. Heart Fail. 9 (12) (2007) 1146–1155, https://doi.org/10.1016/j.ejheart.2007.09.009.

[17] P. Gargiulo, C. Banfi, S. Ghilardi, D. Magri, M. Giovannardi, A. Bonomi, E. Salvioni, E. Battaia, P.P. Filardi, E. Tremoli, P. Agostoni, Surfactant-derived proteins as markers of alveolar membrane damage in heart failure, PLoS One 9 (12) (2014) e115030, , https://doi.org/10.1371/journal.pone.0115030.

[18] L. Regazzoni, L. Del Vecchio, A. Altomare, K.J. Yeum, D. Cusi, F. Locatelli, M. Carini, G. Aldini, Human serum albumin cysteinylation is increased in end stage renal disease patients and reduced by hemodialysis: mass spectrometry studies, Free Radic. Res. 47 (3) (2013) 172–180, https://doi.org/10.3109/10715762.2012.756139.

[19] W.C. Claycomb, N.A. Lanson Jr., B.S. Stallworth, D.B. Egeland, J.B. Delcarpio, A. Bahinski, N.J. Izzo Jr., HL-1 cells: a cardiac muscle cell line that contracts and

retains phenotypic characteristics of the adult cardiomyocyte, Proc. Natl. Acad. Sci. U. S. A. 95 (6) (1998) 2979–2984 https://doi.org/10.1073/pnas.95.6.2979.
[20] M. Brioschi, S. Lento, E. Tremoli, C. Banfi, Proteomic analysis of endothelial cell secretome: a means of studying the pleiotropic effects of Hmg-CoA reductase inhibitors, J Proteomics 78 (2013) 346–361, https://doi.org/10.1016/j.jprot.2012.10.003.
[21] T. Mosmann, Rapid colorimetric assay for cellular growth and survival: application to proliferation and cytotoxicity assays, J. Immunol. Methods 65 (1–2) (1983) 55–63 https://doi.org/10.1016/0022-1759(83)90303-4.
[22] S. Cosentino, C. Banfi, J.C. Burbiel, H. Luo, E. Tremoli, M.P. Abbracchio, Cardiomyocyte death induced by ischaemic/hypoxic stress is differentially affected by distinct purinergic P2 receptors, J. Cell Mol. Med. 16 (5) (2012) 1074–1084, https://doi.org/10.1111/j.1582-4934.2011.01382.x.
[23] M. Roverso, M. Brioschi, C. Banfi, S. Visentin, S. Burlina, R. Seraglia, P. Traldi, A. Lapolla, A preliminary study on human placental tissue impaired by gestational diabetes: a comparison of gel-based versus gel-free proteomics approaches, Eur. J. Mass Spectrom. (Chichester) 22 (2) (2016) 71–82, https://doi.org/10.1255/ejms.1412.
[24] A. Franceschini, D. Szklarczyk, S. Frankild, M. Kuhn, M. Simonovic, A. Roth, J. Lin, P. Minguez, P. Bork, C. von Mering, L.J. Jensen, STRING v9.1: protein-protein interaction networks, with increased coverage and integration, Nucleic Acids Res. 41 (2013) D808–D815, https://doi.org/10.1093/nar/gks1094 (Database issue).
[25] M. Pontremoli, M. Brioschi, R. Baetta, S. Ghilardi, C. Banfi, Identification of DKK-1 as a novel mediator of statin effects in human endothelial cells, Sci. Rep. 8 (1) (2018) 16671, https://doi.org/10.1038/s41598-018-35119-7.
[26] C. Banfi, M. Brioschi, S.S. Barbieri, S. Eligini, S. Barcella, E. Tremoli, S. Colli, L. Mussoni, Mitochondrial reactive oxygen species: a common pathway for PAR1- and PAR2-mediated tissue factor induction in human endothelial cells, J. Thromb. Haemost. 7 (1) (2009) 206–216, https://doi.org/10.1111/j.1538-7836.2008.03204.x.
[27] M. Brioschi, G. Polvani, P. Fratto, A. Parolari, P. Agostoni, E. Tremoli, C. Banfi, Redox proteomics identification of oxidatively modified myocardial proteins in human heart failure: implications for protein function, PLoS One 7 (5) (2012) e35841, , https://doi.org/10.1371/journal.pone.0035841.
[28] S. Lento, M. Brioschi, S. Barcella, M.T. Nasim, S. Ghilardi, S.S. Barbieri, E. Tremoli, C. Banfi, Proteomics of tissue factor silencing in cardiomyocytic cells reveals a new role for this coagulation factor in splicing machinery control, J Proteomics 119 (2015) 75–89, https://doi.org/10.1016/j.jprot.2015.01.021.
[29] K. Terasawa, M. Minami, Y. Minami, Constantly updated knowledge of Hsp90, J. Biochem. 137 (4) (2005) 443–447, https://doi.org/10.1093/jb/mvi056.
[30] C. Kupatt, C. Dessy, R. Hinkel, P. Raake, G. Daneau, C. Bouzin, P. Boekstegers, O. Feron, Heat shock protein 90 transfection reduces ischemia-reperfusion-induced myocardial dysfunction via reciprocal endothelial NO synthase serine 1177 phosphorylation and threonine 495 dephosphorylation, Arterioscler. Thromb. Vasc. Biol. 24 (8) (2004) 1435–1441, https://doi.org/10.1161/01.ATV.0000134300.87476.d1.
[31] W. Wang, Y. Peng, Y. Wang, X. Zhao, Z. Yuan, Anti-apoptotic effect of heat shock protein 90 on hypoxia-mediated cardiomyocyte damage is mediated via the phosphatidylinositol 3-kinase/AKT pathway, Clin. Exp. Pharmacol. Physiol. 36 (9) (2009) 899–903, https://doi.org/10.1111/j.1440-1681.2009.05167.x.
[32] J.D. Jiao, V. Garg, B. Yang, K. Hu, Novel functional role of heat shock protein 90 in ATP-sensitive K+ channel-mediated hypoxic preconditioning, Cardiovasc. Res. 77 (1) (2008) 126–133, https://doi.org/10.1093/cvr/cvm028.
[33] S.W. Chung, J.H. Lee, K.H. Choi, Y.C. Park, S.K. Eo, B.Y. Rhim, K. Kim, Extracellular heat shock protein 90 induces interleukin-8 in vascular smooth muscle cells, Biochem. Biophys. Res. Commun. 378 (3) (2009) 444–449, https://doi.org/10.1016/j.bbrc.2008.11.063.
[34] R. Garcia, D. Merino, J.M. Gomez, J.F. Nistal, M.A. Hurle, A.L. Cortajarena, A.V. Villar, Extracellular heat shock protein 90 binding to TGFbeta receptor I participates in TGFbeta-mediated collagen production in myocardial fibroblasts, Cell. Signal. 28 (10) (2016) 1563–1579, https://doi.org/10.1016/j.cellsig.2016.07.003.
[35] S.S. Guan, M.L. Sheu, R.S. Yang, D.C. Chan, C.T. Wu, T.H. Yang, C.K. Chiang, S.H. Liu, The pathological role of advanced glycation end products-downregulated heat shock protein 60 in islet beta-cell hypertrophy and dysfunction, Oncotarget 7 (17) (2016) 23072–23087, https://doi.org/10.18632/oncotarget.8604.
[36] B.K. Rodino-Janeiro, M. Gonzalez-Peteiro, R. Ucieda-Somoza, J.R. Gonzalez-Juanatey, E. Alvarez, Glycated albumin, a precursor of advanced glycation end-products, up-regulates NADPH oxidase and enhances oxidative stress in human endothelial cells: molecular correlate of diabetic vasculopathy, Diabetes Metab. Res. Rev. 26 (7) (2010) 550–558, https://doi.org/10.1002/dmrr.1117.
[37] C. Ma-On, A. Sanpavat, P. Whongsiri, S. Suwannasin, N. Hirankarn, P. Tangkijvanich, C. Boonla, Oxidative stress indicated by elevated expression of Nrf2 and 8-OHdG promotes hepatocellular carcinoma progression, Med. Oncol. 34 (4) (2017) 57, https://doi.org/10.1007/s12032-017-0914-5.
[38] E. Gianazza, M. Brioschi, A.M. Fernandez, C. Banfi, Lipoxidation in cardiovascular diseases, Redox Biol. (2019) 101119, https://doi.org/10.1016/j.redox.2019.101119.
[39] E. Griesser, V. Vemula, N. Raulien, U. Wagner, S. Reeg, T. Grune, M. Fedorova, Cross-talk between lipid and protein carbonylation in a dynamic cardiomyocyte model of mild nitroxidative stress, Redox Biol. 11 (2017) 438–455, https://doi.org/10.1016/j.redox.2016.12.028.
[40] J. Kim, K.S. Kim, J.W. Shinn, Y.S. Oh, H.T. Kim, I. Jo, S.H. Shinn, The effect of antioxidants on glycated albumin-induced cytotoxicity in bovine retinal pericytes, Biochem. Biophys. Res. Commun. 292 (4) (2002) 1010–1016, https://doi.org/10.1006/bbrc.2002.6751.
[41] M.P. Cohen, E. Shea, S. Chen, C.W. Shearman, Glycated albumin increases oxidative stress, activates NF-kappa B and extracellular signal-regulated kinase (ERK), and stimulates ERK-dependent transforming growth factor-beta 1 production in macrophage RAW cells, J. Lab. Clin. Med. 141 (4) (2003) 242–249, https://doi.org/10.1067/mlc.2003.27.
[42] N.R. Singh, P. Rondeau, L. Hoareau, E. Bourdon, Identification of preferential protein targets for carbonylation in human mature adipocytes treated with native or glycated albumin, Free Radic. Res. 41 (10) (2007) 1078–1088, https://doi.org/10.1080/10715760701487674.
[43] D.J. Gomes, A.P. Velosa, L.S. Okuda, F.B. Fusco, K.S. da Silva, P.R. Pinto, E.R. Nakandakare, M.L. Correa-Giannella, T. Woods, M.A. Brimble, R. Pickford, K.A. Rye, W.R. Teodoro, S. Catanozi, M. Passarelli, Glycated albumin induces lipid infiltration in mice aorta independently of DM and RAS local modulation by inducing lipid peroxidation and inflammation, J. Diabet. Complicat. 30 (8) (2016) 1614–1621, https://doi.org/10.1016/j.jdiacomp.2016.07.001.
[44] K. Aquilano, P. Vigilanza, S. Baldelli, B. Pagliei, G. Rotilio, M.R. Ciriolo, Peroxisome proliferator-activated receptor gamma co-activator 1alpha (PGC-1alpha) and sirtuin 1 (SIRT1) reside in mitochondria: possible direct function in mitochondrial biogenesis, J. Biol. Chem. 285 (28) (2010) 21590–21599, https://doi.org/10.1074/jbc.M109.070169.
[45] J. St-Pierre, S. Drori, M. Uldry, J.M. Silvaggi, J. Rhee, S. Jager, C. Handschin, K. Zheng, J. Lin, W. Yang, D.K. Simon, R. Bachoo, B.M. Spiegelman, Suppression of reactive oxygen species and neurodegeneration by the PGC-1 transcriptional coactivators, Cell 127 (2) (2006) 397–408, https://doi.org/10.1016/j.cell.2006.09.024.
[46] T. Gali Ramamoorthy, G. Laverny, A.I. Schlagowski, J. Zoll, N. Messaddeq, J.M. Bornert, S. Panza, A. Ferry, B. Geny, D. Metzger, The transcriptional coregulator PGC-1beta controls mitochondrial function and anti-oxidant defence in skeletal muscles, Nat. Commun. 6 (2015) 10210, https://doi.org/10.1038/ncomms10210.
[47] S. Baldelli, K. Aquilano, M.R. Ciriolo, PGC-1alpha buffers ROS-mediated removal of mitochondria during myogenesis, Cell Death Dis. 5 (2014) e1515, https://doi.org/10.1038/cddis.2014.458.
[48] Y. Hattori, M. Suzuki, S. Hattori, K. Kasai, Vascular smooth muscle cell activation by glycated albumin (Amadori adducts), Hypertension 39 (1) (2002) 22–28.
[49] H.J. Wang, W.Y. Lo, L.J. Lin, Angiotensin-(1-7) decreases glycated albumin-induced endothelial interleukin-6 expression via modulation of miR-146a, Biochem. Biophys. Res. Commun. 430 (3) (2013) 1157–1163, https://doi.org/10.1016/j.bbrc.2012.12.018.
[50] Y. Liu, C. Liang, X. Liu, B. Liao, X. Pan, Y. Ren, M. Fan, M. Li, Z. He, J. Wu, Z. Wu, AGEs increased migration and inflammatory responses of adventitial fibroblasts via RAGE, MAPK and NF-kappaB pathways, Atherosclerosis 208 (1) (2010) 34–42, https://doi.org/10.1016/j.atherosclerosis.2009.06.007.
[51] Z. Hegab, S. Gibbons, L. Neyses, M.A. Mamas, Role of advanced glycation end products in cardiovascular disease, World J. Cardiol. 4 (4) (2012) 90–102, https://doi.org/10.4330/wjc.v4.i4.90.
[52] E. Selvin, A.M. Rawlings, P.L. Lutsey, N. Maruthur, J.S. Pankow, M. Steffes, J. Coresh, Fructosamine and glycated albumin and the risk of cardiovascular outcomes and death, Circulation 132 (4) (2015) 269–277, https://doi.org/10.1161/CIRCULATIONAHA.115.015415.
[53] K. Esposito, P. Chiodini, M.I. Maiorino, G. Bellastella, A. Capuano, D. Giugliano, Glycaemic durability with dipeptidyl peptidase-4 inhibitors in type 2 diabetes: a systematic review and meta-analysis of long-term randomised controlled trials, BMJ Open 4 (6) (2014) e005442, , https://doi.org/10.1136/bmjopen-2014-005442.